Lymphatic endothelial S1P promotes naïve T cell mitochondrial function and survival

Published in final edited form as:

Nature. 2017 June 01; 546(7656): 158–161. doi:10.1038/nature22352.

Lymphatic endothelial S1P promotes naïve T cell mitochondrial function and survival

Alejandra Mendoza[1], **Victoria Fang**[1], **Cynthia Chen**[1], **Madhavika Serasinghe**[2], **Akanksha Verma**[3], **James Muller**[1], **V. Sai Chaluvadi**[1], **Michael L. Dustin**[1,4], **Timothy Hla**[5], **Olivier Elemento**[3], **Jerry E. Chipuk**[2], and **Susan R. Schwab**[1,*]

[1]Skirball Institute of Biomolecular Medicine, New York University School of Medicine, New York, NY 10016, USA

[2]Department of Oncological Sciences, Icahn School of Medicine at Mount Sinai, New York, NY 10029, USA

[3]Institute for Computational Biomedicine, Weill Cornell Medical College, New York, NY 10021, USA

[4]Kennedy Institute of Rheumatology, University of Oxford, Roosevelt Drive, Headington, Oxford OX3 7FY, UK

[5]Vascular Biology Program, Boston Children's Hospital, Harvard Medical School, Boston, MA 02115, USA

Effective adaptive immune responses require a large naïve T cell repertoire that migrates throughout the body, rapidly identifying virtually any foreign peptide[1]. Because T cell production declines with age, naïve T cells must be long-lived[2]. Yet how naïve T cells survive for years while travelling constantly remains unclear. The chemoattractant sphingosine 1-phosphate (S1P) guides T cell circulation among secondary lymphoid organs – spleen, lymph nodes (LN), and Peyer's patches – where they search for antigen. The concentration of S1P is high in circulatory fluids compared to lymphoid organs, and S1P receptor 1 (S1PR1) directs T cell exit from spleen into blood, and from LN and Peyer's patches into lymph[3]. Here we find that S1P is essential not only for naïve T cell circulation, but also survival. We provide evidence that lymphatic endothelial cells support T cell survival by secreting S1P via the transporter SPNS2, that this S1P signals through S1PR1 on T cells, and that the requirement for S1PR1 is independent of S1PR1's established role in guiding exit from LN. S1P signaling maintains naïve T cell mitochondrial content, providing

*To whom correspondence should be addressed: Susan.Schwab@med.nyu.edu.

Author Contributions

A.M. designed and conducted all experiments, analyzed data, and wrote the manuscript; V.F. performed imaging and image quantification; C.C. performed preliminary experiments with DOP; M.S. performed mitochondrial function experiments; A.V. performed RNA-Seq analysis; J.M. and V.S.C. performed imaging; M.L.D., T.H., O.E., and J.E.C. designed experiments and interpreted data; S.R.S. designed experiments, interpreted data, and wrote the manuscript.

Competing Financial Interests

The authors declare no competing financial interests.

cells energy to continue their constant migration. The S1P signaling pathway is being targeted therapeutically to inhibit autoreactive T cell trafficking, and these findings suggest the possibility of simultaneously targeting autoreactive or malignant cell survival[4].

The transporter SPNS2 is required to supply lymph S1P, but is dispensable for the bulk of blood S1P[5]. In *Spns2*-deficient mice, circulating T cells exit the spleen into blood, but are trapped in LN, resulting in cell redistribution from spleen to LN and a loss of circulating cells[5] (Fig. ED1a). Additionally, *Spns2*-deficient mice have only ~¼ the normal number of naïve T cells in secondary lymphoid organs[5–9]. The loss was widely attributed to defective T cell export from the thymus, where T cells develop. To test this, we deleted *Spns2* using *Lyve1*-Cre. *Lyve1*-Cre efficiently targets lymphatic endothelial cells, which supply the lymph S1P required for T cell exit from LN, but inefficiently targets blood vessel endothelial cells, which regulate T cell exit from the thymus[10]. As expected, T cells in *Spns2*$^{f/f}$*Lyve1*-Cre mice (*Spns2*Δ) left the thymus normally, and redistributed from spleen to LN (Fig. ED1b–f, ED2a–c). However, peripheral T cell numbers were not restored, indicating that the underlying defect was not impaired thymic egress (Fig. 1a, Fig. ED1g). A similar phenotype results from deletion of sphingosine kinases in lymphatic endothelial cells, although the mechanism is unknown[10]. A second possibility for the loss of T cells in *Spns2*Δ mice was that LN were “full” and could not accommodate the cells arriving from the spleen. In that case, T cell numbers should drop in the spleen, and remain steady in LN. In contrast, there was a 2-fold reduction in LN of *Spns2*Δ mice compared to littermate controls (Fig 1b, Fig. ED1h). Naïve T cells were also not found in other tissues, and we saw little evidence of spontaneous activation or reduced homeostatic proliferation (Fig. ED2d–h, ED3).

The one clear defect among naïve T cells in LN of *Spns2*Δ mice was a doubling of the fraction of dying cells, measured by propidium iodide (PI) uptake or by staining with Annexin V and a probe for active caspases (Fig. 1c–e, Fig. ED1i–n). We observed increased death in both *Spns2*Δ mice and *Spns2*Δ mice reconstituted with WT bone marrow (BM), but not WT mice reconstituted with *Spns2*Δ BM, implicating SPNS2 in lymphatic endothelial cells, as opposed to macrophages and other hematopoietic cells targeted by *Lyve1*-Cre (Fig. ED4).

Although the increase in the rate of cell death was modest, it might result in a substantial decline in numbers over time. If increased cell death accounted for the naïve T cell loss, preventing cell death should rescue cell recovery. To test this, we used *BCL2*-transgenic mice, which are resistant to the mitochondrial pathway of apoptosis[11]. We co-transferred *BCL2*-transgenic and WT littermate T cells into *Spns2*Δ mice and littermate controls. Three weeks later, we measured cell recovery. Over-expression of BCL2 did not change the number of T cells recovered in control hosts. Over-expression of BCL2 also did not rescue T cell recovery from spleen of *Spns2*Δ hosts, where T cells are lost because they exit into blood and then become trapped in LN. However, while approximately 35% fewer WT T cells were recovered from LN of *Spns2*Δ mice compared to controls, approximately 60% more *BCL2*-Tg T cells were recovered from LN of *Spns2*Δ mice compared to controls. Upon inhibition of apoptosis, cells accumulated in LN, as we had initially expected to see when cells were trapped there (Fig. 1f, Fig. ED1o,p).

There are many possible explanations for the increased T cell death; indeed, SPNS2 may transport more substrates than S1P. But two changes that T cells in *Spns2*Δ mice experience are: (1) they no longer circulate, and (2) they are exposed to less S1P (they no longer sense S1P periodically in blood and lymph, or low levels of S1P within the LN parenchyma)[12]. We asked whether restoring S1P exposure without restoring circulation could rescue T cell survival. We treated *Spns2*Δ mice and littermate controls with 4-deoxypyridoxine (DOP), which inhibits the S1P-degrading enzyme S1P lyase. DOP increases extracellular S1P in LN of WT mice, and traps T cells in LN by flattening the S1P gradient that drives exit[13]. To confirm that DOP treatment also increased LN S1P in *Spns2*Δ mice, we took advantage of the fact that S1PR1 is internalized upon binding ligand[13, 14]. Surface S1PR1 was 5-fold higher on T cells in vehicle-treated *Spns2*Δ mice than littermate controls, reflecting lower exposure to S1P (Fig. ED5a–c). S1PR1 was internalized on T cells in both DOP-treated control and *Spns2*Δ mice, indicating that S1P exposure had increased (Fig. ED5a–c). In *Spns2*Δ mice, this was due to S1P secretion by cells not targeted by *Lyve1*-Cre or SPNS2-independent secretion. DOP did not restore the S1P gradient required for exit, as there was no increase in circulating T cells in DOP-treated compared to vehicle-treated *Spns2*Δ mice (Fig. ED5d–e). DOP treatment reduced T cell apoptosis and increased the recovery of transferred cells in *Spns2*Δ mice (Fig. 2a–c, Fig. ED5f–h). This suggested that S1P signaling, independent of a role in egress, supports T cell survival.

We next considered whether an S1P receptor controls T cell survival. Naïve T cells express S1PR1 and S1PR4, but we saw no loss of $S1pr4^{-/-}$ T cells in LN (Fig. ED6). A role of S1PR1 in T cell survival has not been addressed because $S1pr1^{-/-}$ T cells do not leave the thymus[15,16]. To test this, we bred mice in which *S1pr1* could be inducibly deleted. We thymectomized adult $S1pr1^{f/f}$*UBC*-CreERT2 mice and littermate controls; then treated both groups with tamoxifen to delete *S1pr1*; and analyzed the mice 12 weeks later. Like *Spns2*Δ mice, *S1pr1*-deficient mice (*S1pr1*Δ; tamoxifen-treated $S1pr1^{f/f}$*UBC*-CreERT2 animals) had a reduction in peripheral naïve T cells and higher frequency of dying naïve T cells (Fig. 3a,b, Fig. ED7a,b). Mixed BM chimeras revealed that the survival defect was T cell-intrinsic (Fig. 3c,d, Fig. ED7c,d). Consistent with a cell-intrinsic role for S1PR1, naïve *S1pr1*Δ T cells isolated from mixed BM chimeras showed down-regulation of transcripts associated with survival and up-regulation of transcripts associated with death (Fig. ED7e). DOP treatment of *S1pr1*Δ mice did not rescue cell death, suggesting that the restored T cell survival in DOP-treated *Spns2*Δ mice was likely mediated by S1PR1 signaling (Fig. ED8).

We next asked how SPNS2/S1P/S1PR1 signaling supports T cell survival. Two extrinsic factors are known to support T cell survival – IL7 and self-peptide/MHC[17–19] – but we found little evidence that S1PR1 signaling regulates access to these (Fig. ED9). This seems unlike the role of CCL19/CCR7 signaling, which also supports T cell survival but does not have an additive effect with loss of IL7 signaling *in vivo*[20].

Naïve T cells rely on oxidative phosphorylation and decline in numbers with mitochondrial dysfunction[21]. We observed a reduction in levels of the mitochondrial proteins VDAC1 and COXIV in *S1pr1*Δ T cells compared to littermate controls (Fig. 4a,b). We further observed a 40% decrease in staining for total mitochondria in *S1pr1*Δ T cells, and a similar decrease in staining for functional mitochondria using MitoTracker CMX-Ros, whose accumulation

depends on mitochondrial membrane potential (Fig. 4c,d, Fig. ED10a). *S1pr1*Δ T cells also had lower oxygen consumption rates (OCR) than littermate controls (Fig. 4e,f, Fig. ED10f). This decrease is unlikely to be secondary to cells undergoing apoptosis, because only a small fraction of cells is detectably apoptotic (Fig. 3b) and because *BCL2*-Tg *S1pr1*Δ T cells have a reduced rate of apoptosis (Fig. ED10b,c) but no increase in respiration (Fig 4f, Fig. ED10d–f). T cells utilize both oxidative phosphorylation and aerobic glycolysis upon activation, and activated *S1pr1*Δ T cells proliferated less than controls when relying primarily on oxidative phosphorylation in medium containing galactose, but similarly to controls when able to perform glycolysis efficiently in the presence of glucose (Fig. ED10g–j)[21,22]. The loss of mitochondria appears specific, as we saw no reproducible decrease in the endoplasmic reticulum (ER) protein calnexin or substantial evidence of ER stress, and the ratio of β-actin to total cell numbers was unchanged (Fig. 4a,b, Fig. ED10k,l). We observed increased deposition of ubiquitin on mitochondria in *S1pr1*Δ T cells, suggesting that mitochondrial loss may be due at least partly to mitophagy (Fig. 4g,h). Consistent with this, *S1pr1*Δ T cells had increased levels of PINK1, a kinase that accumulates upon mitochondrial dysfunction and induces ubiquitination of mitochondrial proteins (Fig. 4i,j)[23]. These data suggest that S1PR1 signaling is required in naïve T cells to maintain mitochondrial content and function.

We identify S1P as an extrinsic factor supporting naïve T cell survival, and suggest a new role for lymphatic endothelial cells in regulating naïve T cell numbers. Although S1PR1 signaling is routinely described as pro-survival, there has been scant evidence that S1PR1 is limiting *in vivo* because mice lacking S1PR1 or both sphingosine kinases die at mid-gestation of hemorrhage[24, 25], confounding attempts to study a cell-intrinsic role of S1PR1 in survival. Studies of S1PR1 in cultured cells are difficult to interpret because S1P in serum is an artificially dominant signal; *in vivo*, cells integrate signaling through multiple receptors sharing common downstream pathways. Consistent with previous reports, S1P induces AKT phosphorylation in LN T cells, and future work will address whether this pathway regulates mitochondrial function (Fig. ED10m)[26]. S1PR1's requirement for naïve T cell survival, in context of the many drugs being developed to target S1PR1 signaling, points to the importance of assessing the requirement for S1PR1 in lymphoma and central memory T cells. Given the energy cost of constant migration to sample antigen, use of the same cue that guides circulation to promote mitochondrial function is an efficient way for naïve T cells to supply their required fuel.

Methods

Mice

Spns2^{f}[5], *S1pr1*^{f}[27], *S1pr4*[28], *Lck-BCL2* transgenic[11], *Lyve1*-Cre[10], *UBC*-CreERT2[29], *UBC-GFP*[30] and MHCII-deficient[31] mice have been previously described. CD45.1^{+} congenic mice were obtained from Charles River Laboratories. All mice were on a C57BL6 or C57BL6-129 background. Mice were 5–52 weeks old at the time of analysis. Male and female mice were used depending on availability, as sex did not appear to affect the results. In all cases mice were compared to littermate controls. Mice were housed in specific pathogen-free conditions at the Skirball Institute animal facility. No animals were excluded

from analysis unless they were clearly sick (hunched, low body weight). These criteria were pre-established, and are standard in the lab. No specific method of randomization was used to allocate mice into groups. The order of sample collection and data acquisition was designed to avoid experimental bias: collection and processing of samples from control and knock-out, as well as treated and untreated animals, were alternated. No blinding was done, as there was no disease scoring. All animal experiments were performed in accordance with protocols approved by the New York University Institutional Animal Care and Use Committee.

Mouse treatments

For bone marrow chimeras, recipients were irradiated with two 6.5 Gray doses of γ irradiation from a cesium source separated by 3 hours, and received 2–10×10^6 bone marrow cells by intravenous injection. Chimeras were analyzed at least 6 weeks after transplantation. Tamoxifen (approximately 75 mg/kg body weight) was administered i.p. on 5 consecutive days. Unless otherwise indicated, analysis was 3 weeks after the last tamoxifen treatment. For adoptive transfer experiments, mice received spleen and LN lymphocytes including 1–3×10^6 naïve CD4 T cells in 0.1 ml by retro-orbital injection. For transfers into MHCII-deficient recipients, 1–3×10^6 naïve CD4 T cells were sorted and labeled with CellTrace Violet (Molecular Probes) according to the manufacturer's instructions before transfer. 4-deoxypyridoxine-HCl (DOP) treated mice received drinking water with 10g/L sucrose plus 30mg/L DOP (Sigma); vehicle-treated mice received drinking water with 10g/L sucrose. Surgical removal of thymi was performed on intubated adult mice under 2% isoflurane using a ventilator (MiniVent Type 845, Harvard Apparatus). For antibody blockade experiments mice were injected i.p. with 0.1 mg of antibodies and analyzed 5 days after injection. For BrdU labeling, 1 mg BrdU (BD Biosciences) in sterile PBS was injected intraperitoneally every 24 hours for 3 days, and mice were analyzed 24 hours after the last injection.

Cell preparation

Lymphocytes were isolated from thymus, spleen, LN, Peyer's patches, lungs, and liver by mechanical disruption and filtration through a 70 μm cell strainer. LN were combined brachial, axillary, inguinal, and mesenteric. Lymphocytes from the small intestinal lamina propria were isolated after removing the Peyer's patches. The tissue was minced with scissors and shaken vigorously for 1 min in HBSS. Minced intestines were further shaken at 100 rpm for 30 minutes at 37C in HBSS containing HEPES (10 mM), sodium pyruvate (1 mM), EDTA (1mM), and DTT (1 mM). Minced pieces were transferred to HBSS containing HEPES (10 mM), sodium pyruvate (1 mM), EDTA (1mM) and shaken at 100 rpm for 10 minutes at 37C minutes to remove the intestinal epithelial lymphocyte fraction (supernatant). Samples were further digested in 0.5 mg/ml Collagenase D (Roche) and 0.1 mg/ml DNAse I in HBSS shaking at 100 rpm at 37C for 20 minutes. Digested samples were filtered through a 40 μm strainer.. Further purification of lymphocytes from the lungs, liver, and lamina propia was performed by density gradient centrifugation using 40% and 80% Percoll (GE Healthcare). The cells at the interphase of the gradient were collected and washed twice.

Macrophages from LN were isolated by thorough mechanical disruption with scissors in HBSS. Minced LN were digested with Collagenase IV (1 mg/ml, Sigma) with DNAse I (0.2

mg/ml, Roche) for 20 minutes in HBSS at 37C with gentle rocking. Digested LN suspensions were passed through a 100 μm cell strainer. Collagenase IV was inactivated with 5 mM EDTA and 10% FBS in PBS.

Further purification, as necessary, was either by magnetic bead enrichment (Stem Cell Technologies, biotin selection kit, used according to the manufacturer's instructions) or flow cytometry (Beckman Coulter MoFlo or BD Biosciences FACSAria). Lymphocytes were enumerated with a cell counter (Beckman Coulter Multisizer 3) set to detect nuclei between 3.5 and 7 μm.

Antibodies

Antibodies to B220 (clone RA3-6B2), CD4 (clone RMA4-5 or GK1.5), CD8 (clone 53-6.7), CD62L (clone MEL14), CD69 (clone H1.2F3), IL7Rα (clone A7R34), CD44 (clone IM7), Nur77 (clone 12.14), Lyve1 (clone ALY7), MHCII (clone M5/114.12.2), gp38 (clone 8.1.1), CD25 (clone PC61), PINK1 (clone 5E1.D8), and rat IgG2a-κ isotype control (clone RTK2758) were purchased from Biolegend, eBiosciences, or BD Biosciences. Anti-S1PR1 (clone 713412) was purchased from R&D Systems. Anti-pSTAT5 (clone D47E7), anti-AKT (catalogue # 9272), anti-pAKT (clone D9E), anti-S6 (clone 5G10) and anti-pS6 (clone D57.2.2E) were purchased from Cell Signaling Technologies. Anti-VDAC1 (clone 20B12AF2) and anti-COXIV **(**clone 20E8C12**)** were purchased from Abcam. Polyclonal anti-calnexin (catalogue #A303-696A) was purchased from Bethyl Laboratories. Polyclonal anti-STAT5 (catalog number C-17) and anti-β–actin (clone C4) were purchased from Santa Cruz Biotechnology. Anti-ubiquitin antibody (clone FK2) was purchased from Enzo Life Sciences. Blocking IL7Rα (clone A7R34)[32] and isotype control (clone 2A3) antibodies were purchased from Bioxcell. AnnexinV and propidium iodide were purchased from Biolegend. CaspACE FITC-VAD-FMK probe for active caspases was purchased from Promega. For flow cytometry, cells were analyzed using an LSRII (BD Biosciences); data were analyzed using FlowJo v. 8.8.1 (Tree Star).

Mitochondrial labeling

Mitochondria were stained using MitoTracker Red CMXRos and MitoTracker Deep Red FM (Life Technologies) according to the manufacturer's instructions. In brief, cells (10E6 cells in 50 μl) were incubated in 2% FBS, 1mM EDTA in PBS containing 0.5 μM MitoTracker dyes along with antibodies for staining cell surface makers for 20 minutes at 37°C. After washing, cells were analyzed using an LSRII (BD Biosciences) or further stained before analysis by confocal microscopy (LSM710; Carl Zeiss).

Microscopy

Confocal imaging was done using standard conditions. In brief, LN were excised, fixed for 1 hour at room temperature in 4% paraformaldehyde, and progressively dehydrated at 4°C in sucrose (10%, 20%, and 30% in PBS). Tissues were snap frozen in OCT compound (Sakura Tissue-Tek). 8 μm tissue sections were cut, rehydrated (rehydration and staining buffer was PBS with 4% mouse serum, 4% rat serum, 10 μg/ml anti-CD16/32, 0.1% Triton X-100), stained, and imaged. Sorted naïve CD4 T cells stained with mitochondrial dyes were adhered to slides by cytospin and fixed in 4% paraformaldehyde for 15 minutes at room

temperature. For ubiquitin stain, cells were permeabilized in 0.1% Triton X-100 for 5 minutes and blocked in 5% casein in PBS for 1 hour at room temperature, followed by antibody staining in 0.1% Triton X-100 with 2% BSA. Nuclei were labeled with DAPI (2 μg/ml). Cells were imaged in mounting media (Life Technologies). All images were acquired using a confocal microscope (LSM710; Carl Zeiss) with a 25X or 63X oil immersion objective. Images were processed and analyzed using ImageJ software (version 1.41; National Institutes of Health).

Colocalization analysis and code availability

To calculate ubiquitin co-localization with mitochondria, pixels positive for the MitoTracker stain were identified, and for each MitoTracker$^+$ pixel the ratio of ubiquitin intensity to MitoTracker intensity was calculated. This ratio was averaged over 3 z-slices per cell. Each point on the graph represents 1 cell. The colocalization program (ImageJ software, version 1.41, National Institutes of Health) used to analyze ubiquitin deposition on mitochondria is provided as Supplementary Text.

In vitro survival assay

Sorted naïve T cells were plated at a density of 10^6 cells per well in 24-well plates and were cultured at 37 °C in RPMI 1640 medium containing HEPES (10 mM) pH 7.2, penicillin (50 IU/ml), streptomycin (50 μg/ml), β-mercaptoethanol (50 μM), 10% FBS, and IL7 (0.01–10 ng/ml) (Peprotech). After 5 days, cells were collected, stained with propidium iodide (Biolegend), and analyzed by flow cytometry.

T cell activation

Freshly isolated LN T cells were stained for 20 min at 37°C with 5 μM CellTrace Violet (Molecular Probes/ThermoFisher) in PBS with 0.1% BSA. 4×10^5 T cells were plated in each well of a 48-well plate, pre-coated with 4 μg/ml anti-CD3 (clone 145-2C11), in activation medium containing 2 μg/mL anti-CD28 (clone 37.51). Activation medium contained glucose-free RPMI 1640 (Gibco) with 10% dialyzed fetal bovine serum (Gibco), 2 mM glutamine (Mediatech), non-essential amino acids (Hyclone), 1 mM sodium pyruvate (Hyclone), and 55 mM 2-mercaptoethanol (Invitrogen), supplemented with either glucose (2 g/L) or galactose (2 g/L). After 72 hours, cells were counted and CellTrace Violet dilution was assayed by flow cytometry.

Western blot

Cells were lysed in RIPA buffer containing phosphatase and protease inhibitor cocktails (Roche). Lysates were resolved by SDS-PAGE followed by Western blot using HRP-conjugated secondary antibodies (Jackson ImmunoResearch Laboratories) and SuperSignal West Pico Chemiluminescent Substrate or SuperSignal West Femto Maximum Sensitivity Chemiluminescent Substrate (Thermo Scientific). Signal was detected using a Chemidoc MP System and quantified using Image Lab software (Bio-Rad Laboratories); there were no saturated pixels in any quantified images. For IL7 stimulation, CD4$^+$ T cells were isolated from LN and stimulated *ex vivo* with IL7 (Peprotech) for 5 minutes at 37°C. For S1P stimulation, CD4 T cells were isolated from LN and incubated *ex vivo* with 1 μM S1P

(Sigma) for 3 hours at 37°C. The cytoplasmic fraction was isolated using NE-PER nuclear and cytoplasmic extraction reagents (Thermo Scientific), according to the manufacturer's instructions.

RNA-Seq

Total RNA was extracted from samples using the RNeasy Plus Mini kit (Life Technologies). Samples were then subject to poly(A) selection using oligo-dT beads (Life Technologies) according to the manufacturer's instructions. RNA samples were used as input for library construction using TotalScript RNA-Seq Kit (Epicentre) according to the manufacturer's instructions. RNA libraries were sequenced on an Illumina HiSeq 2500 (HiSeq Single Read 50 Cycle Lane). Raw sequencing data passed quality control checks performed using FastQC (version 0.11.3). Sequenced reads were aligned to the mouse genome (version mm10 from UCSC) using STAR (version 2.4). Aligned reads were then quantified using HTSeq (version 0.6.0) for raw counts and CuffLinks (version 2.2.1) for FPKM against the UCSC mm10 reference annotation. Initial expression data clustering revealed a batch effect due to variation between experimental days. The expression was corrected for batch effects using R package ComBat (Bioconductor Release 3.3) and a two-factor analysis for genotype and experimental day. R package Limma (Bioconductor Release 3.3) was used to identify differentially expressed genes. Genes significantly differentially expressed with a Benjamini-Hochberg adjusted p-value <0.05 (FDR=0.05) were selected. Pathway analysis on these genes was performed using Ingenuity Pathway Analysis (Qiagen, version 1.0). We show genes that fall into Ingenuity Pathway Analysis' "Molecular and Cellular Functions" category, with the annotation "Cell death and survival." Heat maps were created using batch-corrected expression values that were log-normalized (log2[Expression +1]) using ggplot2 library in R (Bioconductor Release 3.3).

Mitochondrial function

Mitochondrial function of sorted naïve T cells was assessed using Seahorse XF Cell Mito Stress Test Kit (Agilent Technologies) according to the manufacturer's instructions. In brief, sorted naïve T cells were plated in Seahorse XF Base Medium supplemented with 1 mM pyruvate, 2 mM glutamine, and 10 mM glucose (pH 7.4) in Seahorse XF96 Cell Culture microwell plates coated with CellTak (Corning). Cells were incubated for 45 minutes at 37°C without CO_2 before running the assay. Samples were then run on a Seahorse XF^e96 Extracellular Flux Analyzer (Agilent Technologies) using the Seahorse XF Cell Mito Stress Test kit with 1 μM Oligomycin, 1 μM FCCP, and 0.5 μM Rotenone/Antimycin A. All samples were run in duplicate or triplicate. Equivalent cell numbers per sample were confirmed post-run by analyzing DNA content.

RT-qPCR

Total RNA was extracted from sorted cell populations using TRIzol (Invitrogen) according to the manufacturer's instructions. Before reverse transcription, RNA was treated with DNase I (Invitrogen). The RNA was converted to cDNA with Invitrogen's Superscript III First Strand Synthesis System according to the manufacturer's instructions, using a mix of oligo dT and random hexamers as primers. Real-time quantitative PCR (qPCR) was

performed on a Roche Light-Cycler 480 using iQ SYBR Green Supermix (Bio-Rad) according to the manufacturer's instructions. Primer pairs used were:

Hprt F AGGTTGCAAGCTTGCTGGT;

Hprt R TGAAGTACTCATTATAGTCAAGGGCA;

Eif2ak3 F GTGCTTACAGTGGAAAGCTGAG;

Eif2ak3 R GAAGTTCAAAGTGGCCAACACT;

Hspa5 F CTGCTGAGGCGTATTTGGGA;

Hspa5 R GCAGCTGCTGTAGGCTCATT;

Ddit3 F GGAACCTGAGGAGAGAGTGTTC;

Ddit3 R CGTCTCCAAGGTGAAAGGCA.

To control for DNA contamination, a reaction without reverse transcriptase was performed in parallel for each sample/primer pair. To control for nonspecific amplification, the size of the reaction products was analyzed by agarose gel electrophoresis. Primer pairs were tested for linear amplification over two orders of magnitude.

Statistics

All comparisons are by Student's 2-tailed unpaired t-test, except comparisons of protein abundance by Western blot, which are by Student's 2-tailed paired t-test. When data are plotted on a log-scale, log-transformed data are compared. For all graphs, bars or lines indicate mean and error bars indicate SEM. Sample sizes were chosen based on our experience with mouse models. In the case of negative results, we do not exclude the possibility that a difference would have been revealed with a larger sample size.

Data Availability

RNA-Seq data has been deposited with NIH/NCBI as GEO dataset GSE97249.

Extended Data

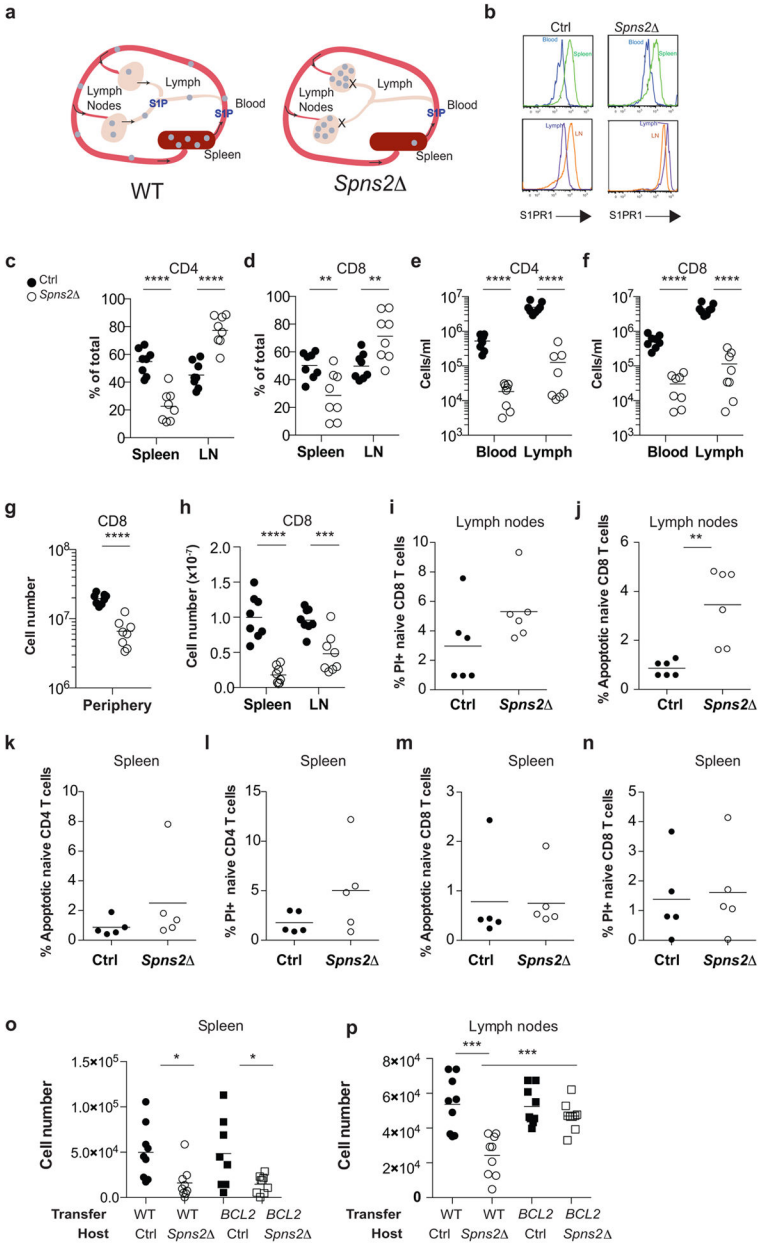

Extended Data Figure 1. SPNS2 is required in lymphatic endothelial cells for peripheral T cell circulation

(a) Diagram of distribution of naïve T cells in the periphery of *Spns2*Δ mice and controls. *Spns2*Δ mice have normal plasma S1P and egress from the spleen into blood proceeds as usual, but in *Spns2*Δ mice lymph S1P is lost and egress from lymph nodes is blocked. Over time, this leads to a redistribution of T cells from spleen to lymph nodes and a loss of circulating cells, because any cell that leaves the spleen and enters a lymph node is trapped. **(b)** Representative surface S1PR1 on naïve $CD4^+$ T cells in the blood and spleen (top panels) and in the lymph and LN (bottom panels) of a *Spns2*Δ mouse and its littermate

control (Ctrl). Surface S1PR1 on T cells is internalized upon binding S1P. Hence the lower S1PR1 on the surface of T cells in blood than spleen, in both *Spns2*Δ and control animals, indicates that T cells sense more S1P in blood than spleen. S1PR1 is also lower on the surface of T cells in lymph than LN of control mice. But in *Spns2*Δ mice S1PR1 is equally high on T cells in lymph and LN, suggesting that the gradient that directs T cell exit from LN has been ablated. **(c–h)** T cell distribution in *Spns2*Δ mice and littermate controls. **(c–d)** Percent of total peripheral naïve CD4 **(c)** and CD8 **(d)** T cells in the spleen and LN. Total peripheral lymphocytes are defined as those in spleen and a subset of LN (brachial, axillary, inguinal, and mesenteric); blood and lymph make a negligible contribution. **(e–f)** Number of naïve CD4 **(e)** and CD8 **(f)** T cells in blood and lymph. **(g)** Total number of naïve CD8 T cells in the periphery. **(h)** Naïve CD8 T cell numbers in the spleen and LN. Data in **(b–h)** are representative of or pool 8 pairs of mice analyzed in 8 experiments. **(i–j)** Frequency of PI^+ **(i)** and apoptotic **(j)** naïve CD8 T cells in LN of *Spns2*Δ mice and littermate controls. 6 pairs of mice analyzed in 6 experiments. **(k–n)** Frequency of apoptotic **(k,m)** and PI^+ **(l,n)** naïve CD4 T cells **(k,l)** and CD8 T cells **(m,n)** in spleen of *Spns2*Δ mice and littermate controls. 5 pairs of mice analyzed in 5 experiments. There is no statistically significant difference in death of naïve CD4 or CD8 T cells in the spleen of *Spns2*Δ mice compared to littermate controls, although there seems to be a trend towards increased death in *Spns2*Δ mice. Normal T cell survival in the spleen of *Spns2*Δ mice is consistent with normal blood S1P and normal S1P production by blood vessel endothelial cells lining the marginal sinus, which likely maintain normal S1PR1 signaling in T cells in the spleen. We hypothesize that the few T cells able to leave the LN of *Spns2*Δ mice are relatively healthy, and stabilized while they are in the spleen. However, we hesitate to over-interpret these results because very few T cells remain in the spleen of *Spns2*Δ animals, and they may be different in a way that is not captured by gating on $CD62L^{hi}CD44^{lo}$ T cells. **(o–p)** Congenically labeled lymphocytes from *BCL2*-Tg and WT littermate donors were co-transferred (1:1 by naïve CD4 counts) to *Spns2*Δ mice and littermate controls. Number of WT or *BCL2*-Tg naïve CD8 T cells recovered in spleen and LN 21 days after transfer. 9 pairs of mice analyzed in 3 experiments. Lines indicate mean. Unpaired 2-tailed t-test, *p<0.05, **p<0.01, ***p<0.001 ****p<0.0001.

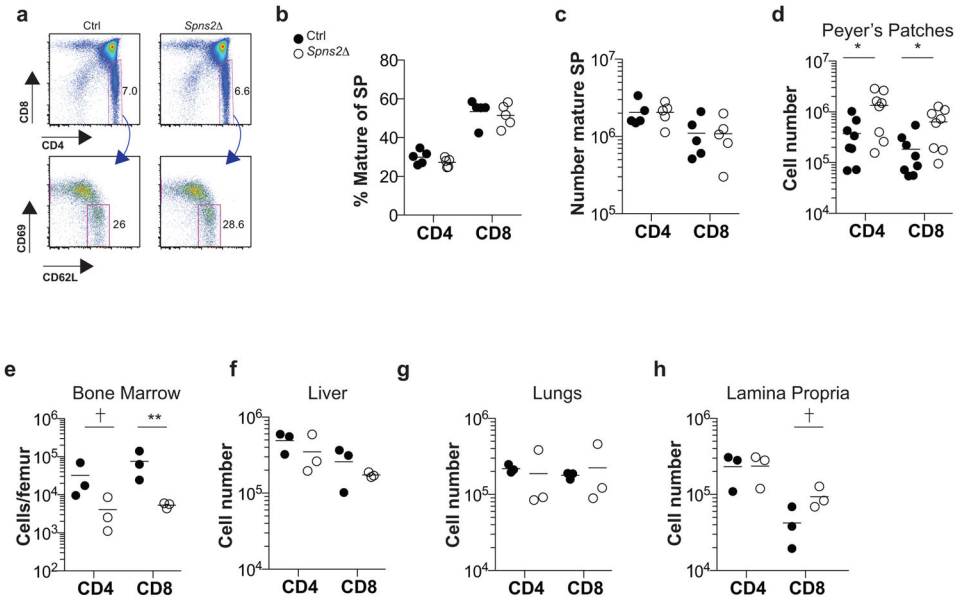

Extended Data Figure 2. *Spns2* deletion in lymphatic endothelial cells does not block thymic egress, and does not induce substantial accumulation of naïve T cells in tissues other than LN and spleen

A reduction in the efficiency of T cell exit from the thymus is reflected in an accumulation of mature ($CD69^{low}CD62L^{hi}$) single positive (SP) T cells. **(a)** Expression of CD4 and CD8 by total thymocytes (upper panels), and expression of CD69 and CD62L by CD4SP thymocytes (lower panels), from a representative *Spns2*Δ mouse and littermate control. **(b)** Percent mature CD4SP of total CD4SP and percent mature CD8SP of total CD8SP T cells in *Spns2*Δ mice and littermate controls. **(c)** Number of mature CD4SP and CD8SP thymocytes in *Spns2*Δ mice and littermate controls. Graphs in **(b–c)** compile 5 pairs of mice analyzed in 5 experiments. **(d–e)** Number of naïve CD4 and CD8 T cells in the Peyer's patches **(d)** and bone marrow **(e)** of *Spns2*Δ mice and littermate controls. **(f–h)** Number of CD4 and CD8 T cells in liver **(f)**, lungs **(g)** and small intestine lamina propria **(h)** of *Spns2*Δ mice and littermate controls. Interestingly, T cells do accumulate in the Peyer's patches of *Spns2*Δ mice, but the numbers account for only ~5% of the missing cells (there were ~ 2.1E7 fewer naïve CD4 T cells in the combined spleen, mesenteric, inguinal, brachial, and axillary LN of *Spns2*Δ mice compared to controls, and 9.6E5 more naïve CD4 T cells in the Peyer's patches of *Spns2*Δ mice compared to controls). Graph in (**d)** pools 8 pairs of mice analyzed in 8 experiments, and **(e–h)** pool 3 pairs of mice analyzed in 3 experiments. Lines indicate mean. Unpaired 2-tailed t-test, $^{\dagger}p=0.07$ for **(e)**, $^{\dagger}p=0.095$ for **(h)**, *p<0.05, **p<0.01.

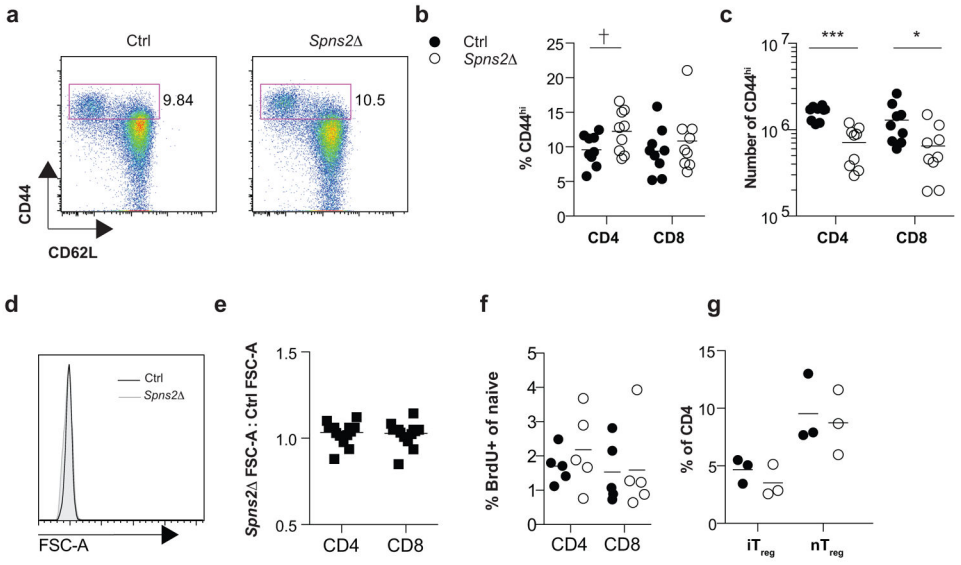

Extended Data Figure 3. Loss of naïve T cells in *Spns2*Δ mice is not due to conversion to another cell type

To assess whether T cells in *Spns2*Δ mice lose quiescence and die of activation-induced apoptosis, we assessed CD44 expression, cell size, and BrdU incorporation. **(a)** Expression of CD44 and CD62L on CD4 T cells in LN of representative *Spns2*Δ and littermate control mice. **(b)** % $CD44^{hi}$ of total CD4 and % $CD44^{hi}$ of total CD8 T cells in LN. **(c)** Number of $CD44^{hi}CD4^{+}$ T cells and $CD44^{hi}CD8^{+}$ T cells in LN. Data in **(b–c)** pool 9 pairs of mice analyzed in 9 experiments. **(d)** Forward scatter area (FSC-A) of naïve CD4 T cells in LN of a representative *Spns2*Δ (shaded) and littermate control (black) mouse. **(e)** Ratio of mean FSC-A of naive CD4 and CD8 T cells in the LN of a *Spns2*Δ mouse to mean FSC-A of naïve CD4 and CD8 T cells in the LN of its littermate control. Data pool 16 pairs of mice analyzed in 16 experiments. **(f)** Mice were injected intraperitoneally with BrdU daily for 3 days. 24 hours after the last injection, LN were collected and naïve CD4 and CD8 T cells were analyzed by flow cytometry for BrdU incorporation. Data pool 5 pairs of mice analyzed in 5 experiments. **(g)** Frequencies of induced regulatory T cells (iTreg) and natural regulatory T cells (nTreg) in the LN of *Spns2*Δ and littermate control mice. iTreg were defined as $FOXP3^{+}Neuropilin^{-}$ and nTreg were defined as $FOXP3^{+}Neuropilin^{+}$. Data pool 3 pairs of mice analyzed in 3 experiments. Lines indicate mean. Unpaired 2-tailed t-test, $^{\dagger}p=0.051$, $*p<0.05$, $p***<0.001$.

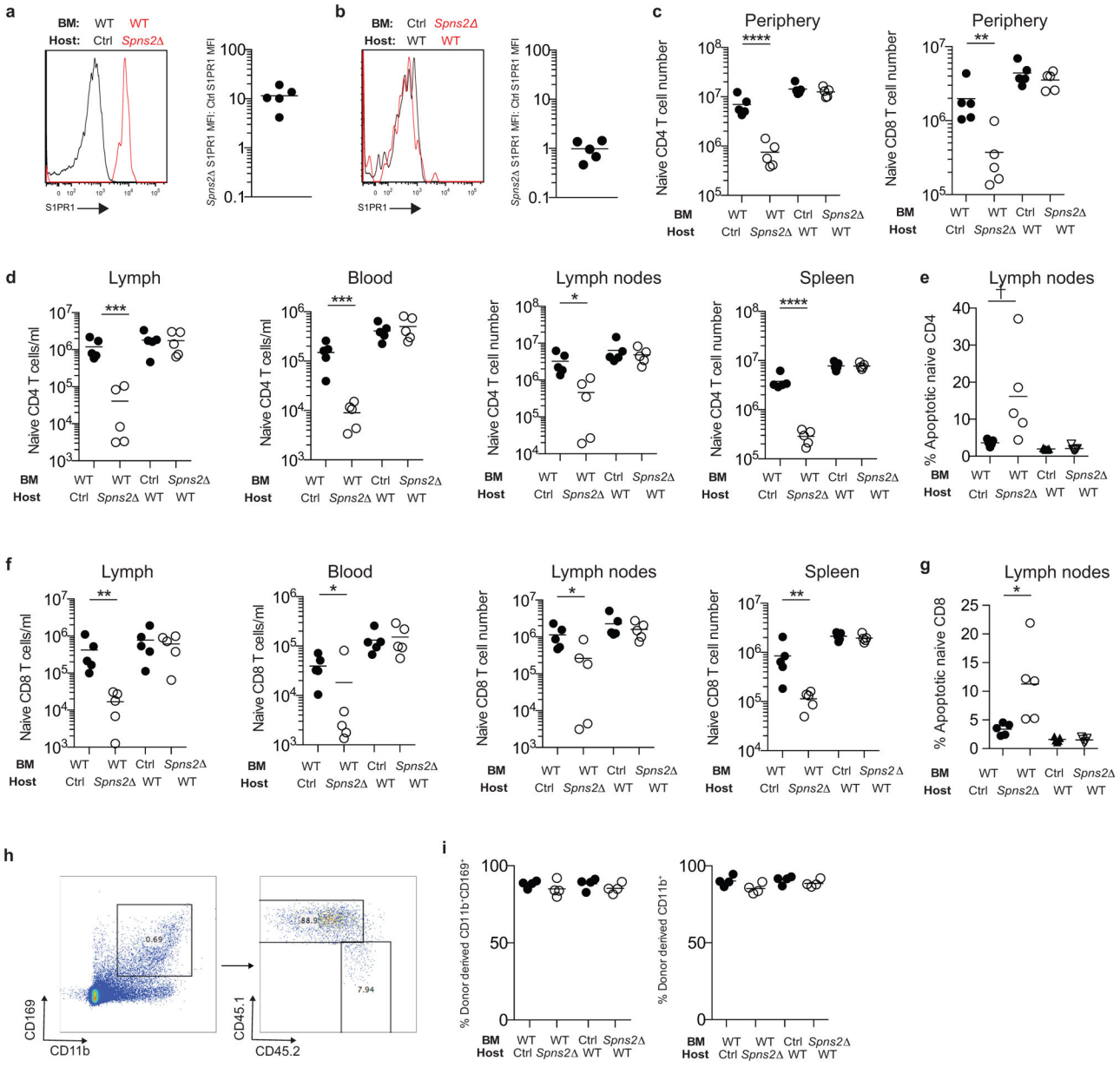

Extended Data Figure 4. *Spns2* is required in *Lyve1*-Cre deleted radioresistant cells

Hosts were lethally irradiated and reconstituted with bone marrow (BM) from the specified congenically-marked donors. Mice were analyzed > 6 weeks after transplantation. **(a)** Representative flow cytometry plot of surface S1PR1 on T cells in lymph of the indicted chimeras (left). Ratio of surface S1PR1 MFI on naïve T cells in the lymph of a *Spns2*Δ mouse reconstituted with WT BM to surface S1PR1 MFI on naïve T cells in the lymph of a littermate control with WT BM (right). Graph compiles 5 pairs of mice analyzed in 5 experiments. **(b)** Representative flow cytometry plot of surface S1PR1 on T cells in lymph of the indicted chimeras (left). Ratio of surface S1PR1 MFI on naïve T cells in the lymph of a WT mouse reconstituted with *Spns2*Δ BM to surface S1PR1 MFI on naïve T cells in the lymph of a WT mouse reconstituted with littermate control BM (right). Graph compiles 5

pairs of mice analyzed in 5 experiments. **(c)** Total number of donor-derived naïve CD4 and CD8 T cells in the periphery (combined spleen and mesenteric, axillary, inguinal, and brachial LN) of the indicated chimeras. **(d)** Number of donor-derived naïve CD4 T cells in the lymph, blood, LN and spleen of the indicated chimeras. **(e)** Frequency of apoptotic donor-derived naïve CD4 T cells in the LN of the indicated chimeras. **(f)** Number of donor-derived naïve CD8 T cells in the lymph, blood, LN and spleen of the indicated chimeras. **(g)** Frequency of apoptotic donor-derived naïve CD8 T cells in the LN of the indicated chimeras. **(c–g)** compile 5 sets of mice (made using 2 pairs of *Spns2*Δ and control donors and 2 WT donors) analyzed in 5 experiments. **(h–i)** Reconstitution of macrophages in the LN of chimeras. **(h)** Gating scheme to assess reconstitution in bulk $CD11b^+$ cells and $CD11b^+CD169^+$ sinus-lining macrophages. Representative plots for 4 sets of mice analyzed in 4 experiments. **(i)** Quantification of percent donor-derived $CD11b^+$ and $CD11b^+CD169^+$ macrophages. The average percent donor-derived $CD45^+$ hematopoietic cells was 92%, $CD11b^+$ macrophages was 89%, and $CD11b^+CD169^+$ macrophages was 87%. Graphs compile 4 sets of mice (made using 2 pairs of *Spns2*Δ and control donors and 2 WT donors) analyzed in 4 experiments. Lines indicate mean. Unpaired 2-tailed t-test, $^{\dagger}p=0.061$, $^{*}p<0.05$, $^{**}p<0.01$, $^{***}p<0.001$, $^{****}p<0.0001$.

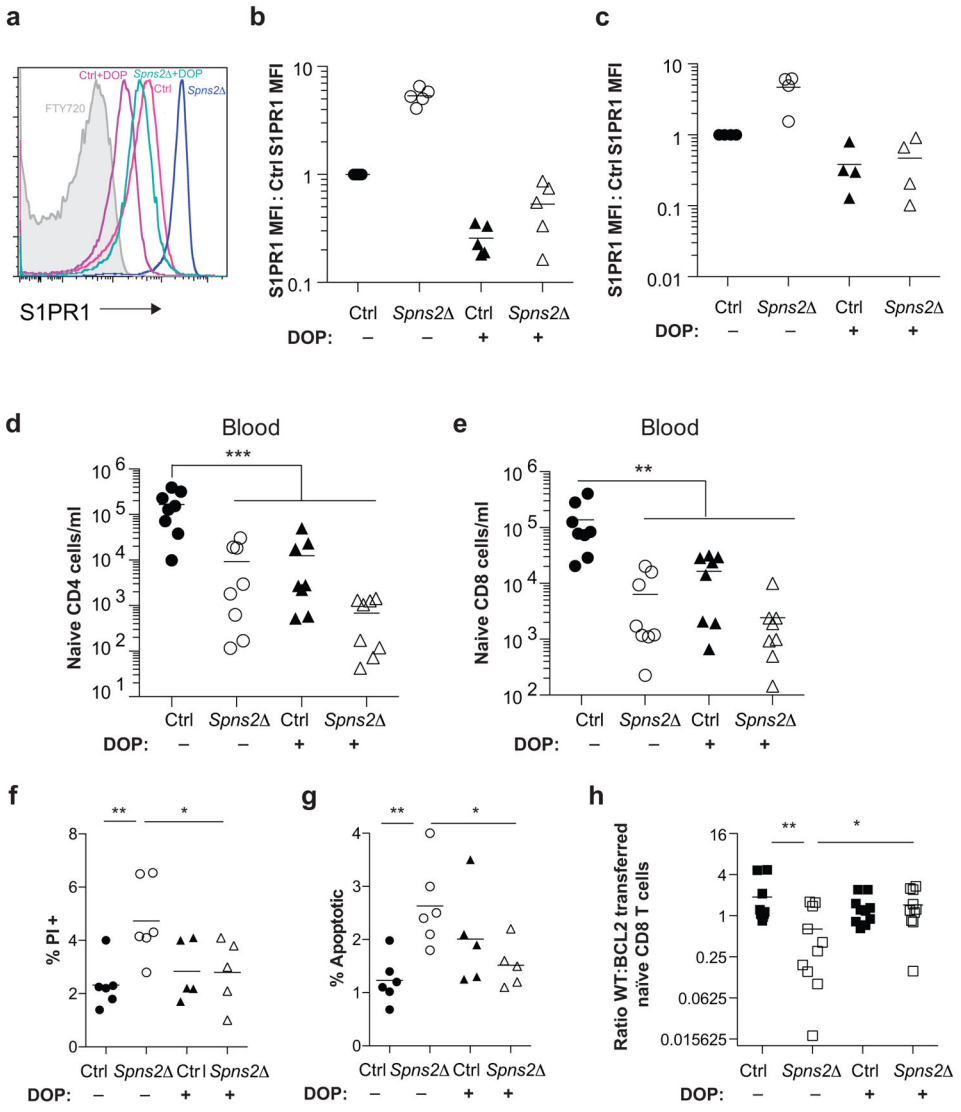

Extended Data Figure 5. Naïve T cell survival is dependent on S1P, but independent of circulation

*Spns2*Δ mice and littermate controls were treated for 21 days with 30 mg/L DOP and 10 g/L sucrose, or sucrose alone, in the drinking water. **(a–c)** The effect of DOP treatment on T cell exposure to extracellular S1P within the LN was assessed by measuring surface expression of S1PR1 on naïve T cells, which is inversely related to S1P levels. **(a)** Representative flow cytometry plot of surface S1PR1 on naïve CD4 T cells. An FTY720-treated mouse was used as a negative control for S1PR1 staining. **(b)** Ratio of cell surface S1PR1 mean fluorescence intensity (MFI) on naïve LN CD4 T cells from the indicated mice to cell surface S1PR1 MFI on naïve LN CD4 T cells from sucrose-treated control mice. 5 groups of mice analyzed in 5 experiments. **(c)** Ratio of cell surface S1PR1 MFI on naïve LN CD8 T cells from the indicated mice to cell surface S1PR1 MFI on naïve LN CD8 T cells from sucrose-treated control mice. 4 groups of mice analyzed in 4 experiments. **(d–e)** Number of naïve CD4 **(d)** or CD8 **(e)** T cells in the blood of *Spns2*Δ mice and littermate controls, with and without DOP treatment. 8 groups of mice analyzed in 5 experiments. **(f–g)** Frequency of PI^+ **(f)** and

apoptotic **(g)** naïve CD8 T cells in LN of *Spns2*Δ mice and littermate controls, with and without DOP treatment. 5 groups (control and *Spns2*Δ groups had a total of 6 mice, DOP-treated control and DOP-treated *Spns2*Δ groups had a total of 5 mice) analyzed in 3 experiments. **(h)** Congenically marked *BCL2*-Tg and littermate WT lymphocytes (at a 1:1 ratio for naïve CD4 T cell counts) were co-transferred to *Spns2*Δ and littermate control mice, with and without DOP treatment. 21 days after transfer, WT or *BCL2*-Tg naïve CD8 T cells recovered in LN were enumerated. Ratio of WT to *BCL2*-Tg T cells is shown for control and DOP-treated *Spns2*Δ mice and littermate controls. 10 mice per group of recipients analyzed in 4 experiments. Lines indicate mean. Unpaired 2-tailed t-test, *p<0.05, **p<0.01, ***p<0.001.

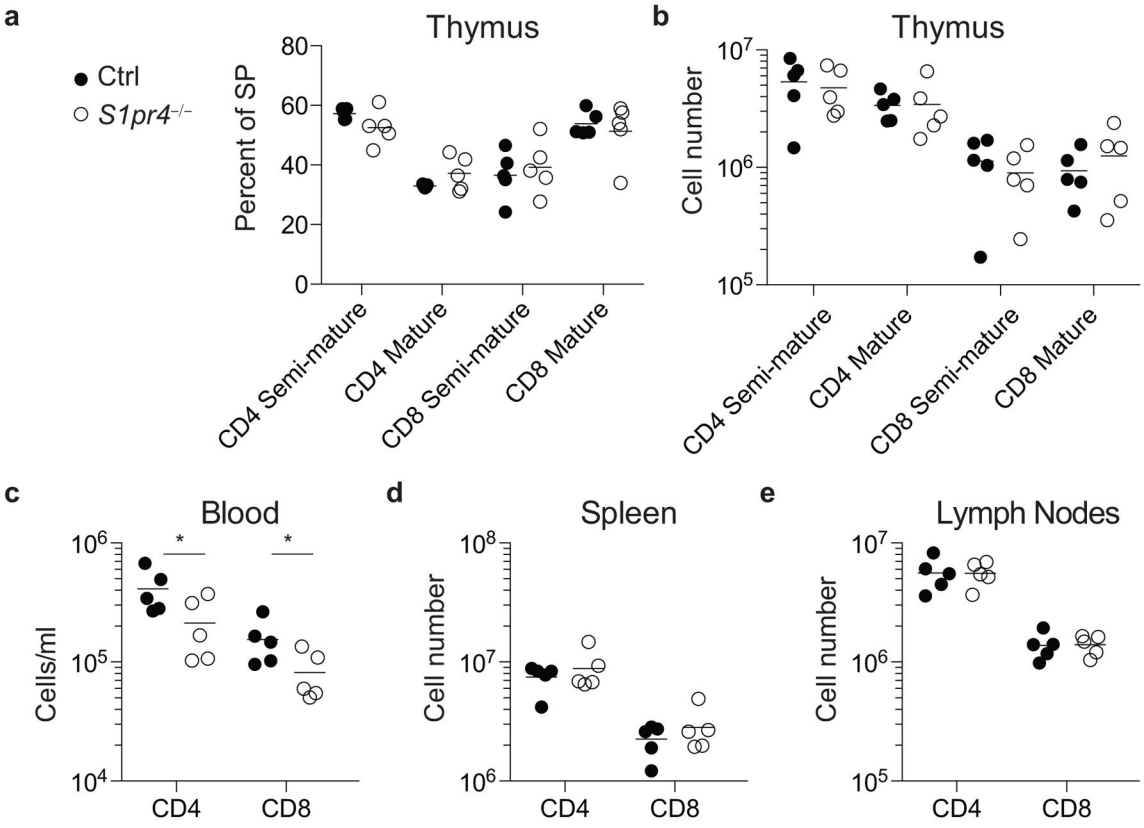

Extended Data Figure 6. Naïve T cell survival is not dependent on S1PR4 signaling

WT CD45.1$^+$ mice were lethally irradiated and reconstituted with bone marrow from CD45.2$^+$ *S1pr4*$^{-/-}$ or littermate control mice. Mice were analyzed 6 weeks after bone marrow reconstitution. **(a)** Percent semi-mature (CD69^{hi}CD62L^{lo}) and mature (CD69^{lo}CD62L^{hi}) of total CD4SP thymocytes and percent semi-mature and mature of total CD8SP thymocytes in *S1pr4*$^{-/-}$ and control chimeras. **(b)** Number of semi-mature and mature CD4SP and CD8SP thymocytes. **(c–e)** Number of naïve CD4 and CD8 T cells in blood **(c)**, spleen **(d)** and LN **(e)**. LN quantified were brachial, axillary, inguinal, and mesenteric. Two sets of *S1pr4*$^{-/-}$ and littermate control bone marrow donors were used. Data pool 5 pairs of chimeras analyzed in 3 experiments, all gated on CD45.2$^+$ cells. Lines indicate mean. Unpaired 2-tailed t-test, *p<0.05.

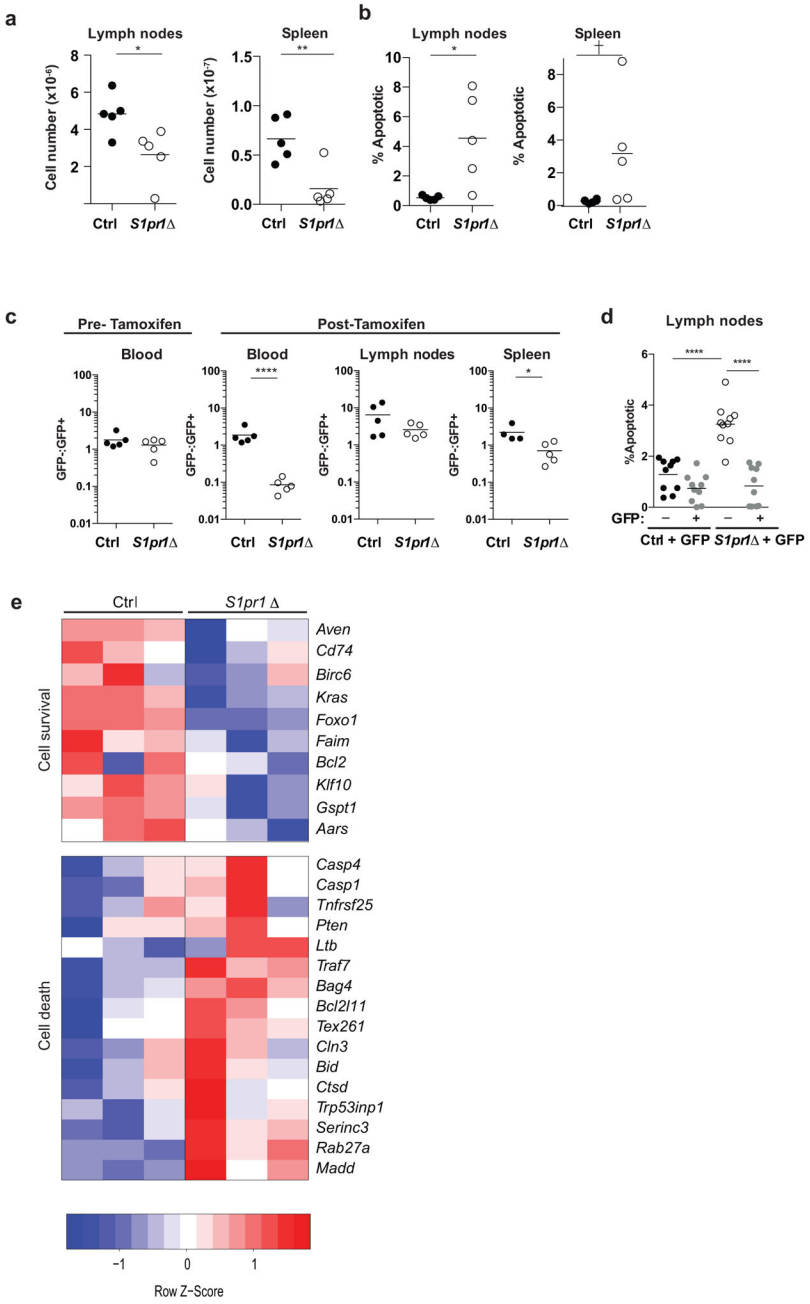

Extended Data Figure 7. Cell autonomous S1PR1 signaling is required in naïve CD8 T cells to inhibit apoptosis

(a–b) Adult *S1pr1*$^{f/f}$*UBC*-CreERT2 mice and littermate controls were thymectomized, treated with tamoxifen, and analyzed 12 weeks later (tamoxifen-treated *S1pr1*$^{f/f}$*UBC*-CreERT2 mice are referred to as *S1pr1*Δ). **(a)** Number of naïve CD8 T cells in LN (mesenteric, axillary, inguinal, and brachial) and spleen of *S1pr1*Δ mice and littermate controls. **(b)** Frequency of apoptotic naïve CD8 T cells in LN and spleen of *S1pr1*Δ mice and littermate controls. 5 pairs of mice analyzed in 3 experiments. **(c–d)** CD45.1^{+} mice were lethally irradiated and reconstituted with a mix of BM from WT *UBC:GFP* mice and BM

from *S1pr1*$^{f/f}$*UBC*-CreERT2 CD45.2^{+} mice or littermate controls. The mice were thymectomized 6 weeks after reconstitution and tamoxifen treated 4 weeks after surgery. **(c)** Ratio of the number of *S1pr1*$^{f/f}$*UBC*-CreERT2 or littermate control naïve CD8 T cells to the number of GFP^{+} naïve CD8 T cells found in the blood before tamoxifen-induced *S1pr1* deletion, and the same ratio in the blood, LN, and spleen 24 weeks after tamoxifen treatment. 5 pairs of mice from 2 bone marrow donor sets (except control spleen, with 4 mice), analyzed in 3 experiments. **(d)** Frequency of apoptotic *S1pr1*Δ or littermate control naïve CD8 T cells and GFP^{+} WT naïve CD8 T cells. 10 pairs of mice from 3 bone marrow donor sets analyzed in 5 experiments 12 or 24 weeks after tamoxifen treatment. **(e)** CD45.1^{+} WT mice were irradiated and reconstituted with a 1:1 ratio of *UBC:GFP* WT BM and either CD45.2^{+} *S1pr1*$^{f/f}$ *or S1pr1*$^{f/f}$*;UBC*-CreERT2 BM. After 6 weeks, Cre activity was induced with 5 daily injections of tamoxifen (in both groups of mice). 5 days after the last dose of tamoxifen, naive GFP^{-}CD45.2^{+} CD4 T cells were sorted from LN. Transcripts were quantified by RNA-Seq, and differentially expressed genes (Benjamini-Hochberg adjusted p-value <0.05) were analyzed using Ingenuity Pathway Analysis (Qiagen v. 1.0). Differentially expressed transcripts that fell into the “Molecular and Cellular Functions” category with the annotation “Cell death and survival” are shown. Lines indicate mean. Unpaired 2-tailed t-test, †p=0.092, *p<0.05, **p<0.01, **** p<0.0001.

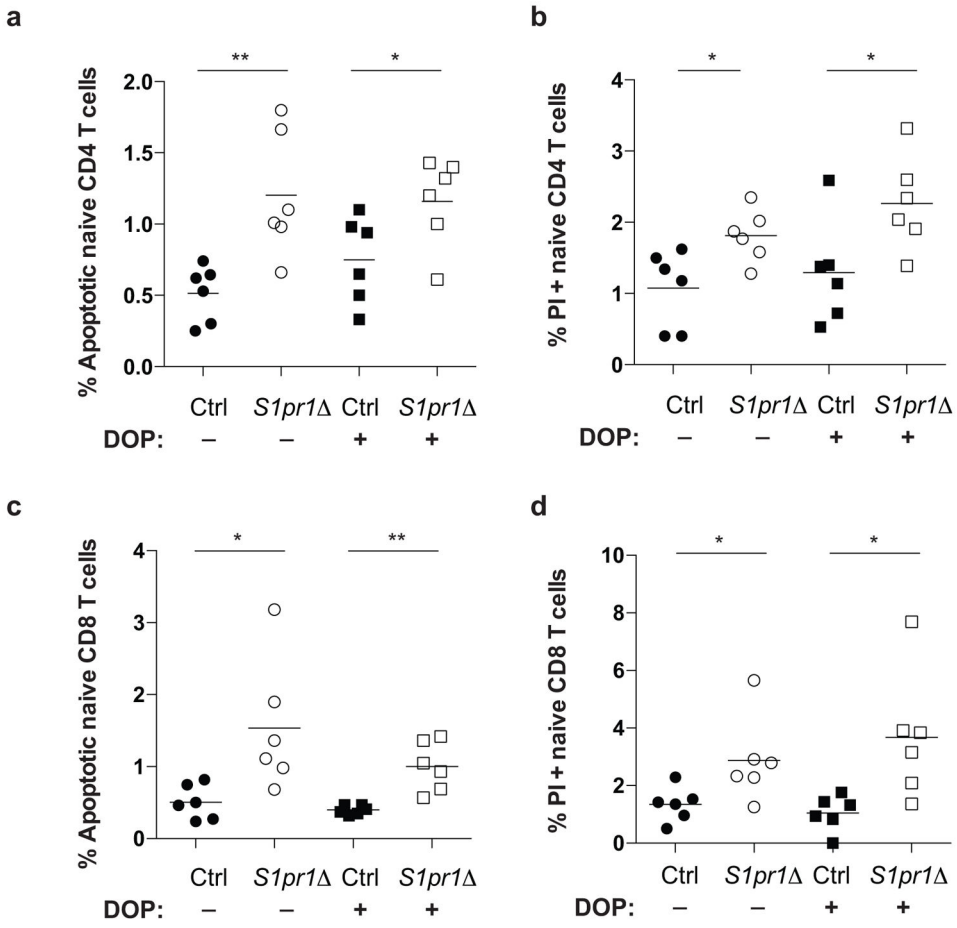

Extended Data Figure 8. DOP does not rescue cell death in *S1pr1* deficient mice

Frequency of apoptotic **(a, c)** and PI^+ **(b, d)** naïve CD4 **(a, b)** and naïve CD8 **(c, d)** T cells in LN of *S1pr1*Δ mice and littermate controls, with and without DOP treatment (30 mg/L DOP with 10 g/L sucrose in drinking water, or sucrose alone, for 3 weeks, as in Fig. 2). 6 groups of mice analyzed in 4 experiments. Lines indicate mean. Unpaired 2-tailed t-test, *p<0.05, **p<0.01.

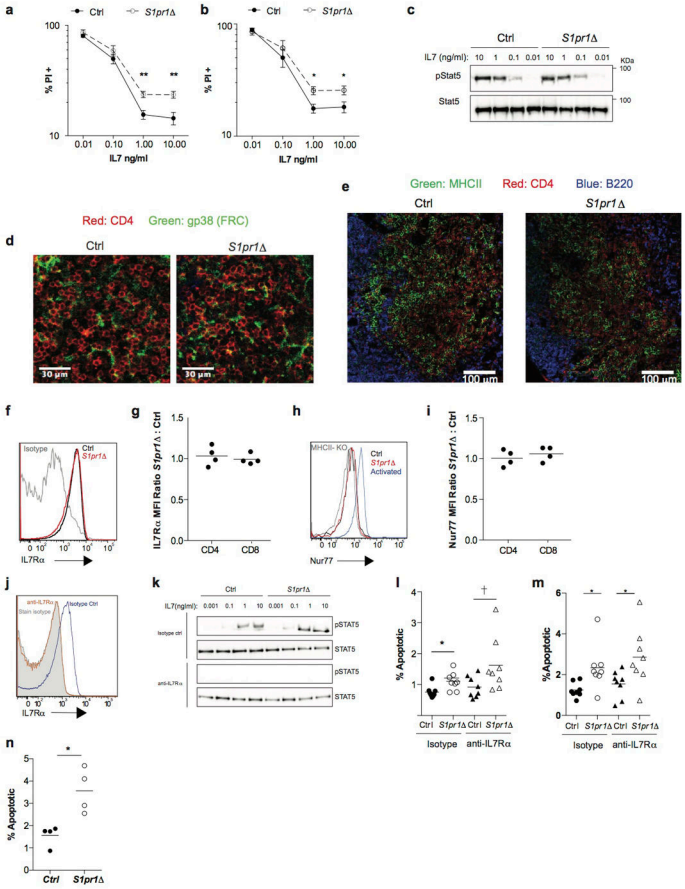

Extended Data Figure 9. Little evidence that S1PR1 regulates access to IL7 or self-peptide/MHC

(a–b) Sorted naïve CD4 T cells (which do not express MHCII) **(a)** and sorted naïve CD8 T cells **(b)** from LN of *S1pr1*Δ and littermate control animals were cultured for 5 days in the indicated concentrations of IL7. Frequency of PI^+ cells measured by flow cytometry. Graph pools 9 experiments (a) or 6 experiments (b). **(c)** Western blot of LN CD4 T cells stimulated *ex vivo* with IL7. Representative of 2 experiments. **(d–e)** Immunofluorescence staining for the indicated markers in the LN T zone. (FRC, fibroblastic reticular cells). Representative of 3 experiments. **(f)** Representative cell surface IL7Rα on LN naïve CD4 T cells. **(g)** Ratio of IL7Rα MFI on *S1pr1*Δ LN naïve CD4 and CD8 T cells to littermate controls. Compiles data from 4 pairs in 4 experiments. **(h)** Representative Nur77 expression by naïve CD4 T cells isolated from LN of *S1pr1*Δ and littermate control animals. Naïve CD4 T cells transferred to MHCII-KO recipients and activated CD4 T cells were used as negative and positive controls for Nur77 expression respectively. **(i)** Ratio of Nur77 MFI in *S1pr1*Δ LN naïve T cells to

littermate controls. Graph compiles 4 pairs of mice analyzed in 4 experiments. **(j–m)** *S1pr1*Δ and littermate control mice were treated with either IL7Rα blocking or isotype control antibody, and analyzed 5 days later. **(j)** Efficacy of IL7Rα blockade was assessed by staining for IL7Rα (using the anti-IL7Rα blocking antibody) on naïve CD4 T cells from LN of mice treated with anti-IL7Rα and isotype control. **(k)** Efficacy of IL7Rα blockade was measured by the ability of LN CD4 T cells from anti-IL7Rα and isotype control treated mice to phosphorylate STAT5 in response to IL7 *ex vivo* (5 minute stimulation with the indicated concentrations of IL7), measured by Western blot. Representative of 3 experiments. **(l–m)** Frequency of apoptotic naïve CD4 **(l)** and CD8 **(m)** T cells in LN. 8 groups of mice analyzed in 4 experiments. **(n)** Sorted LN naïve CD4 T cells from *S1pr1*Δ animals and littermate controls were transferred to MHCII-KO recipients. Cells in recipient LN were analyzed 5 days later. 4 pairs in 4 experiments. We cannot exclude effects below our limit of detection, or the possibility that pre-existing defects in *S1pr1*Δ cells preserve the differences measured in our assays. Lines mean, error bars SEM. Unpaired 2-tailed t-test, †=0.052, *p<0.05, **p<0.01.

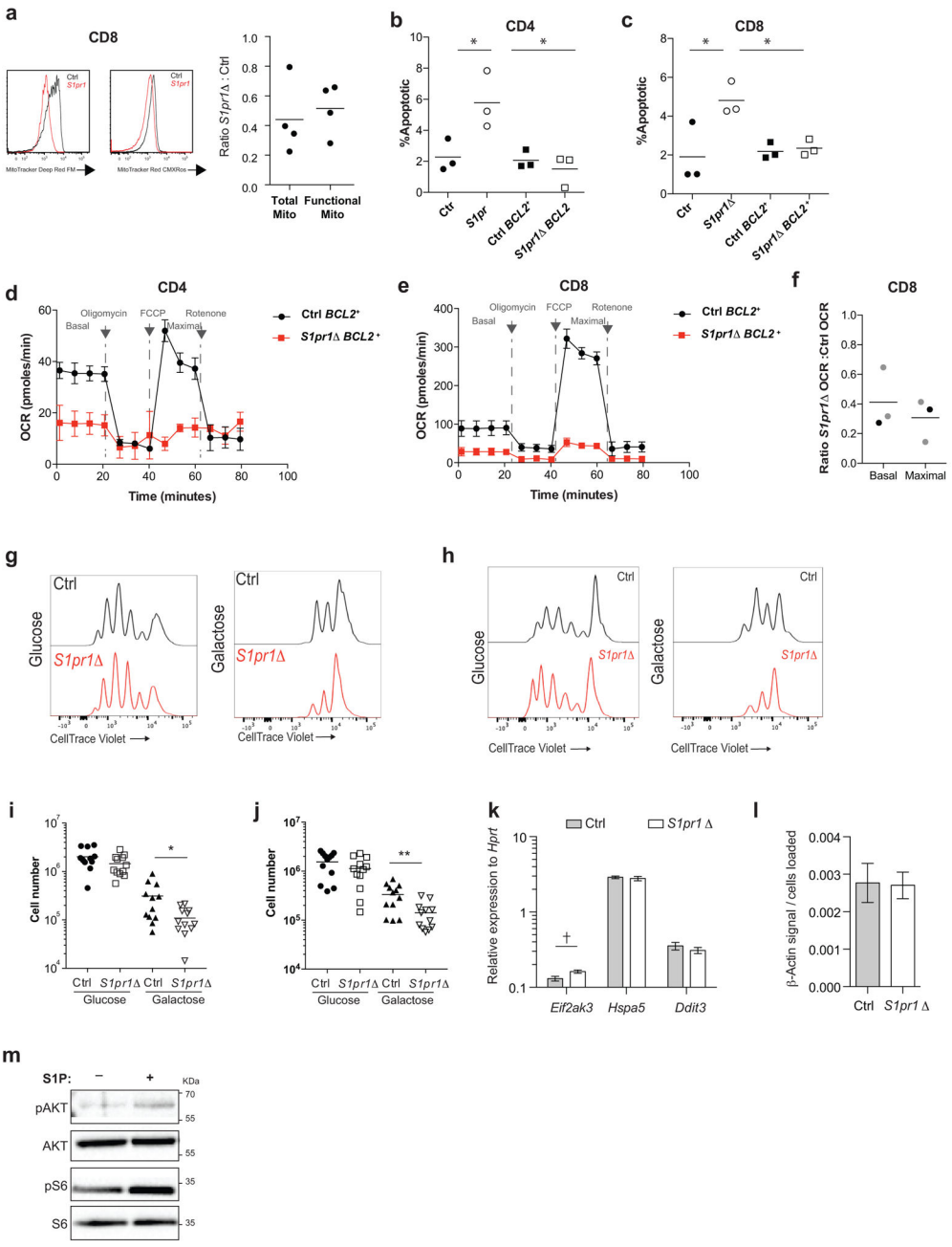

Extended Data Figure 10. Naïve T cells require S1PR1 signaling for maintenance of mitochondrial content and function

(a) Naïve CD8 T cells from LN of *S1pr1*Δ mice and littermate controls were analyzed by flow cytometry for total mitochondria (MitoTracker Deep Red FM) and functional mitochondria (MitoTracker Red CMX-Ros). Representative histograms and compiled ratios are shown for 4 pairs of mice analyzed in 4 experiments. **(b–c)** Frequency of apoptotic naïve CD4 **(b)** or CD8 **(c)** T cells from LN of Ctrl, *S1pr1*Δ, Ctrl *BCL2*$^{+}$, and *S1pr1*Δ *BCL2*$^{+}$ mice. Compiles 3 sets of mice analyzed in 3 experiments. **(d–e)** Mitochondrial function was assayed *ex vivo* in sorted naïve CD4 and CD8 T cells from LN of Ctrl *BCL2*$^{+}$ and *S1pr1*Δ

BCL2^{+} mice using XF Cell Mito Stress Test Kit and an XF^{e}96 Extracellular Flux Analyzer (Agilent Technologies, formerly Seahorse). **(d)** Oxygen consumption rate (OCR) of naïve CD4 T cells from LN of Ctrl *BCL2*$^{+}$ and *S1pr1*Δ *BCL2*$^{+}$mice. Graph plots replicates from 1 experiment. Error bars show SEM. Data are representative of 2 pairs of mice analyzed in 2 experiments. **(e)** OCR of naïve CD8 T cells from Ctrl *BCL2*$^{+}$ and *S1pr1*Δ *BCL2*$^{+}$mice. Graph plots replicates from 1 experiment. Error bars show SEM. Data are representative of 2 pairs of mice analyzed in 2 experiments. **(f)** Ratio of average basal and maximal oxygen consumption rates (OCR) of *S1pr1*Δ naïve CD8 LN T cells to the average basal and maximal OCR of littermate controls. Graph compiles 3 pairs of mice analyzed in 3 experiments. Black dots indicate OCR ratios between *S1pr1*Δ mice and controls, grey dots indicate OCR ratios between *S1pr1*Δ*;BCL2*-tg mice and *BCL2*-tg controls. **(g–j)** CellTrace Violet-labeled CD4 and CD8 T cells from LN of *S1pr1*Δ mice and littermate controls were activated with anti-CD3/CD28 and cultured in medium supplemented with glucose or galactose for 72 hours. CellTrace Violet dilution for CD4 **(g)** and CD8 **(h)** T cells and total numbers of CD4 **(i)** and CD8 **(j)** T cells measured 72 hours after activation. Graph compiles triplicate samples from 4 pairs of mice analyzed in 4 experiments. **(k)** Transcripts upregulated as part of the ER unfolded protein response – *Eif2ak3* (PERK), *Hspa5* (BIP), *and Ddit3* (CHOP) – were measured by RT-qPCR on sorted naïve CD4 T cells from LN of *S1pr1*Δ and littermate control animals. Data compile 4 sets of cells sorted from 4 pairs of mice. Error bars show SEM. **(l)** Ratio of β-actin signal quantified by Western blot to the number of CD4 T cells loaded per well from *S1pr1*Δ mice and littermate controls. Graph compiles 4 sets of samples from 4 pairs of mice analyzed in 2 experiments (a subset of the samples in Fig. 4b). **(m)** CD4 T cells isolated from LN were stimulated *ex vivo* with 1 μM S1P or vehicle for 3 hours. AKT and S6 phosphorylation were assessed by Western blot. Representative of 2 experiments. Lines and bars mean, error bars SEM. Unpaired 2-tailed t-test, † =p=0.053, *p<0.05, **p<0.01.

Supplementary Material

Refer to Web version on PubMed Central for supplementary material.

Acknowledgments

We thank members of the Schwab and Sfeir labs for discussions, Thomas Trimarchi for help analyzing RNA-Seq data, Richard Proia for *S1pr4*$^{-/-}$ mice, Sandra Milasta for advice on glucose/galactose activation, and Agnel Sfeir for critical reading of the manuscript. This work was supported by NIH R01 AI085166 and AI123308 to S.R.S.; NIH R01 CA206005, an American Cancer Society Research Scholar Grant, and a Leukemia & Lymphoma Society Career Development Award to J.E.C.; US National Science Foundation CAREER grant 1054964 and NCI R01 CA194547 to O.E.; NIH R01 HL089934 to T.H.; NIH R37 AI43542 to J.M. for M.L.D; and NIH T32 AI100853 to A.M., V.F, and C.C.

References

1. Jenkins MK, Chu HH, McLachlan JB, Moon JJ. On the composition of the preimmune repertoire of T cells specific for Peptide-major histocompatibility complex ligands. Annual review of immunology. 2010; 28:275–294.
2. Boehm T, Swann JB. Thymus involution and regeneration: two sides of the same coin? Nature reviews. Immunology. 2013; 13:831–838.

3. Cyster JG, Schwab SR. Sphingosine-1-phosphate and lymphocyte egress from lymphoid organs. Annual review of immunology. 2012; 30:69–94.
4. Proia RL, Hla T. Emerging biology of sphingosine-1-phosphate: its role in pathogenesis and therapy. The Journal of clinical investigation. 2015; 125:1379–1387. [PubMed: 25831442]
5. Mendoza A, et al. The transporter Spns2 is required for secretion of lymph but not plasma sphingosine-1-phosphate. Cell reports. 2012; 2:1104–1110. [PubMed: 23103166]
6. Fukuhara S, et al. The sphingosine-1-phosphate transporter Spns2 expressed on endothelial cells regulates lymphocyte trafficking in mice. The Journal of clinical investigation. 2012; 122:1416–1426. [PubMed: 22406534]
7. Hisano Y, Kobayashi N, Yamaguchi A, Nishi T. Mouse SPNS2 Functions as a Sphingosine-1-Phosphate Transporter in Vascular Endothelial Cells. PloS one. 2012; 7:e38941. [PubMed: 22723910]
8. Nagahashi M, et al. Spns2, a transporter of phosphorylated sphingoid bases, regulates their blood and lymph levels, and the lymphatic network. FASEB journal : official publication of the Federation of American Societies for Experimental Biology. 2013; 27:1001–1011. [PubMed: 23180825]
9. Nijnik A, et al. The role of sphingosine-1-phosphate transporter spns2 in immune system function. Journal of immunology. 2012; 189:102–111.
10. Pham TH, et al. Lymphatic endothelial cell sphingosine kinase activity is required for lymphocyte egress and lymphatic patterning. The Journal of experimental medicine. 2010; 207:17–27. S11–14. [PubMed: 20026661]
11. Sentman CL, Shutter JR, Hockenbery D, Kanagawa O, Korsmeyer SJ. bcl-2 inhibits multiple forms of apoptosis but not negative selection in thymocytes. Cell. 1991; 67:879–888. [PubMed: 1835668]
12. Fang V, et al. Gradients of the signaling lipid S1P in lymph nodes position natural killer cells and regulate their interferon-gamma response. Nature immunology. 2017; 18:15–25. [PubMed: 27841869]
13. Schwab SR, et al. Lymphocyte sequestration through S1P lyase inhibition and disruption of S1P gradients. Science. 2005; 309:1735–1739. [PubMed: 16151014]
14. Liu CH, et al. Ligand-induced trafficking of the sphingosine-1-phosphate receptor EDG-1. Mol Biol Cell. 1999; 10:1179–1190. [PubMed: 10198065]
15. Matloubian M, et al. Lymphocyte egress from thymus and peripheral lymphoid organs is dependent on S1P receptor 1. Nature. 2004; 427:355–360. [PubMed: 14737169]
16. Allende ML, Dreier JL, Mandala S, Proia RL. Expression of the sphingosine 1-phosphate receptor, S1P1, on T-cells controls thymic emigration. The Journal of biological chemistry. 2004; 279:15396–15401. [PubMed: 14732704]
17. Takada K, Jameson SC. Naive T cell homeostasis: from awareness of space to a sense of place. Nature reviews. Immunology. 2009; 9:823–832.
18. Chang JE, Turley SJ. Stromal infrastructure of the lymph node and coordination of immunity. Trends in immunology. 2015; 36:30–39. [PubMed: 25499856]
19. Surh CD, Sprent J. Homeostasis of naive and memory T cells. Immunity. 2008; 29:848–862. [PubMed: 19100699]
20. Link A, et al. Fibroblastic reticular cells in lymph nodes regulate the homeostasis of naive T cells. Nature immunology. 2007; 8:1255–1265. [PubMed: 17893676]
21. Milasta S, et al. Apoptosis-Inducing-Factor-Dependent Mitochondrial Function Is Required for T Cell but Not B Cell Function. Immunity. 2016
22. Chang CH, et al. Posttranscriptional control of T cell effector function by aerobic glycolysis. Cell. 2013; 153:1239–1251. [PubMed: 23746840]
23. Pickrell AM, Youle RJ. The roles of PINK1, parkin, and mitochondrial fidelity in Parkinson's disease. Neuron. 2015; 85:257–273. [PubMed: 25611507]
24. Liu Y, et al. Edg-1, the G protein-coupled receptor for sphingosine-1-phosphate, is essential for vascular maturation. The Journal of clinical investigation. 2000; 106:951–961. [PubMed: 11032855]

25. Mizugishi K, et al. Essential role for sphingosine kinases in neural and vascular development. Mol Cell Biol. 2005; 25:11113–11121. [PubMed: 16314531]

26. Liu G, et al. The receptor S1P1 overrides regulatory T cell-mediated immune suppression through Akt-mTOR. Nature immunology. 2009; 10:769–777. [PubMed: 19483717]

27. Allende ML, Yamashita T, Proia RL. G-protein-coupled receptor S1P1 acts within endothelial cells to regulate vascular maturation. Blood. 2003; 102:3665–3667. [PubMed: 12869509]

28. Allende ML, et al. Sphingosine-1-phosphate lyase deficiency produces a pro-inflammatory response while impairing neutrophil trafficking. The Journal of biological chemistry. 2011; 286:7348–7358. [PubMed: 21173151]

29. Ruzankina Y, et al. Deletion of the developmentally essential gene ATR in adult mice leads to age-related phenotypes and stem cell loss. Cell stem cell. 2007; 1:113–126. [PubMed: 18371340]

30. Schaefer BC, Schaefer ML, Kappler JW, Marrack P, Kedl RM. Observation of antigen-dependent CD8+ T-cell/ dendritic cell interactions in vivo. Cellular immunology. 2001; 214:110–122. [PubMed: 12088410]

31. Madsen L, et al. Mice lacking all conventional MHC class II genes. Proceedings of the National Academy of Sciences of the United States of America. 1999; 96:10338–10343. [PubMed: 10468609]

32. Sudo T, et al. Expression and function of the interleukin 7 receptor in murine lymphocytes. Proceedings of the National Academy of Sciences of the United States of America. 1993; 90:9125–9129. [PubMed: 8415665]

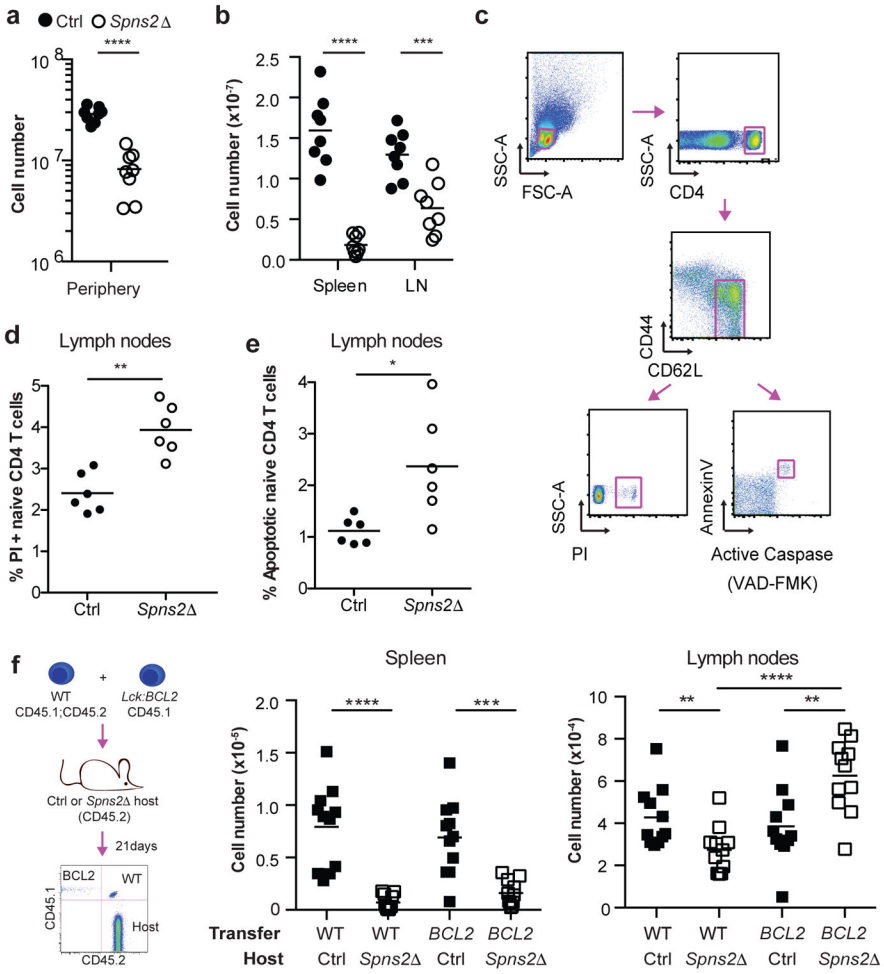

Figure 1. SPNS2 is required for naïve T cell survival

(a,b) Number of naïve ($CD44^{low}CD62L^{hi}$) CD4 T cells in periphery (combined spleen and LN) **(a)**, spleen, and LN **(b).** 8 pairs analyzed in 8 experiments. **(c–e)** Gating **(c)** and frequency of PI^{+} **(d)** and apoptotic **(e)** LN naïve CD4. 6 pairs, 6 experiments. **(f)** Congenically-labeled lymphocytes from *BCL2*-Tg and WT littermates were co-transferred (1:1 by naïve CD4 counts). 21 days later, naïve CD4 were enumerated in recipients' tissues. 11 pairs, 4 experiments. t-test, *p<0.05, **p<0.01, ***p<0.001, ****p<0.0001.

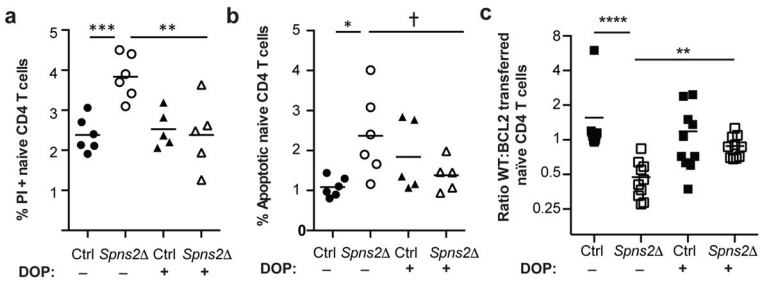

Figure 2. Naïve T cell survival depends on S1P, but not circulation

*Spns2*Δ mice and littermate controls were treated for 21 days with DOP or vehicle. Frequency of PI^+ **(a)** and apoptotic **(b)** LN naïve CD4. 5 groups, 3 experiments. **(c)** Congenically marked *BCL2*-Tg and littermate WT lymphocytes were co-transferred (1:1 by naïve CD4 counts). 21 days later, naïve CD4 were enumerated in recipients' LN. 10 groups, 4 experiments. t-test, $^{\dagger}p=0.078$, *p<0.05, **p<0.01, ***p<0.001, ****p<0.0001.

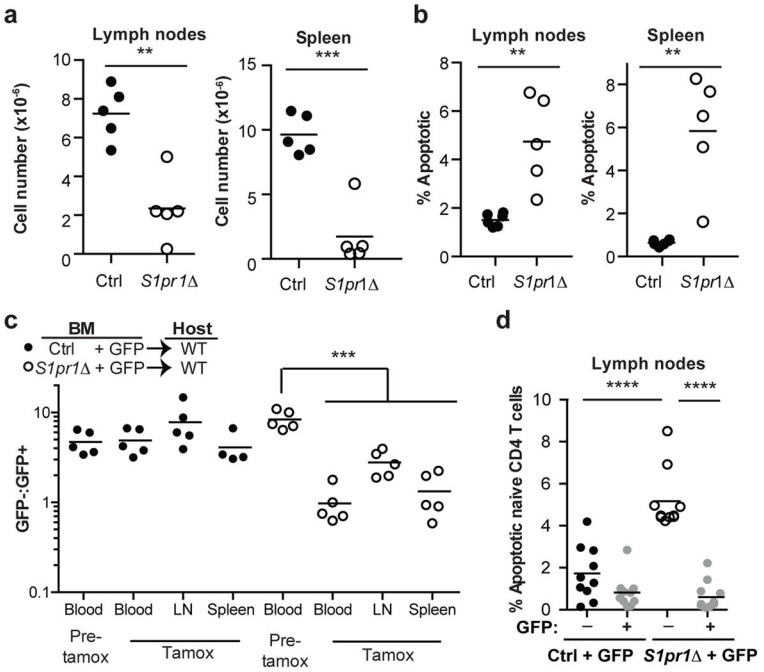

Figure 3. Cell-autonomous S1PR1 inhibits apoptosis

(a–b) Adult *S1pr1*$^{f/f}$*UBC*-CreERT2 mice and littermate controls were thymectomized, tamoxifen-treated, and analyzed 12 weeks later. Number of naïve CD4 **(a)**, and frequency of apoptotic naïve CD4 **(b)**. 5 pairs, 3 experiments. **(c–d)** CD45.1^{+} mice were reconstituted with a mix of BM from WT *UBC:GFP* mice and BM from *S1pr1*$^{f/f}$*UBC*-CreERT2 CD45.2^{+} mice or littermate controls. Chimeras were thymectomized 6 weeks after reconstitution, and tamoxifen-treated 4 weeks later. **(c)** Ratio of the number of *S1pr1*$^{f/f}$*UBC*-CreERT2 or control naïve CD4 to GFP^{+} naïve CD4. 5 pairs of mice from 2 BM donor sets, analyzed in 3 experiments 24 weeks post-tamoxifen (control spleen has 4 mice). **(d)** Frequency of apoptotic naïve CD4 in LN. 10 pairs from 3 BM donor sets in 5 experiments analyzed 12 or 24 weeks post-tamoxifen. t-test, **p<0.01, ****p<0.0001.

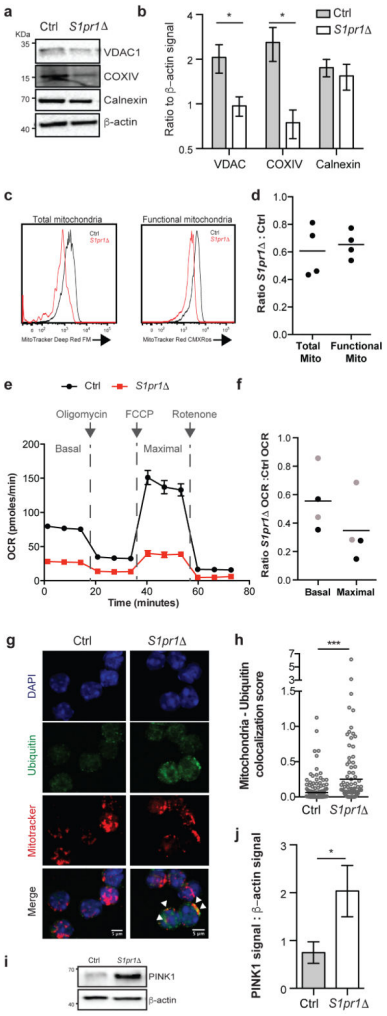

Figure 4. Naïve T cells require S1PR1 to maintain mitochondrial content

(a–b) LN CD4 T cells analyzed by Western blot. Quantification of 7 pairs in 5 experiments for VDAC1 and calnexin, 6 pairs in 5 experiments for COXIV. **(c–d)** LN naïve CD4 analyzed by flow cytometry. 4 pairs, 4 experiments. **(e–f)** OCR of sorted LN naïve CD4. Curve showing technical replicates from one pair **(e)**, and compilation of 4 pairs in 3 experiments **(f)**. Black dots indicate ratios between *S1pr1*Δ and controls, grey dots ratios between *S1pr1*Δ*;BCL2*-tg and *BCL2*-tg controls. **(g–h)** Immunofluorescence of LN CD4 T cells. Arrows, examples of colocalization. Quantification compiles cells from 7 pairs in 6 experiments. **(i–j)** LN CD4 T cells analyzed by Western blot. 6 pairs, 4 experiments. Error, SEM. t-test, *p<0.05, ***p<0.001.